Article

Developmental Cell

Kinesin 1 Drives Autolysosome Tubulation

Highlights

- KIF5B drives autolysosome tubulation by pulling on the autolysosomal membrane
- Clathrin promotes formation of PtdIns(4,5)P_2-enriched microdomains on autolysosomes
- KIF5B directly interacts with PtdIns(4,5)P_2
- KIF5B clusters on PtdIns(4,5)P_2-enriched microdomains in a clathrin-dependent manner

Authors

Wanqing Du, Qian Peter Su, Yang Chen, ..., Lingfei Sun, Yujie Sun, Li Yu

Correspondence

sun_yujie@pku.edu.cn (Y.S.), liyulab@mail.tsinghua.edu.cn (L.Y.)

In Brief

During autophagy, lysosomes fuse with autophagosomes to create autolysosomes. Lysosomes are later regenerated via a process involving autolysosome tubulation. Du et al. show that the KIF5B kinesin, through interactions with PtdIns(4,5)P_2, drives tubulation by pulling on the autolysosome membrane, revealing a motor-based membrane deformation process that helps maintain lysosomal homeostasis.

Du et al., 2016, Developmental Cell *37*, 326–336
May 23, 2016
http://dx.doi.org/10.1016/j.devcel.2016.04.014

CellPress

CellPress

Developmental Cell
Article

Kinesin 1 Drives Autolysosome Tubulation

Wanqing Du,[1,4,5] Qian Peter Su,[2,5] Yang Chen,[1,5] Yueyao Zhu,[1] Dong Jiang,[1] Yueguang Rong,[1] Senyan Zhang,[1] Yixiao Zhang,[1] He Ren,[3] Chuanmao Zhang,[3] Xinquan Wang,[4] Ning Gao,[4] Yanfeng Wang,[4] Lingfei Sun,[4] Yujie Sun,[2,3,*] and Li Yu[1,*]

[1]State Key Laboratory of Membrane Biology, Tsinghua University-Peking University Joint Center for Life Sciences, School of Life Sciences, Tsinghua University, Beijing 100084, China

[2]State Key Laboratory of Membrane Biology, Biodynamic Optical Imaging Center (BIOPIC), School of Life Sciences, Peking University, Beijing 100871, China

[3]School of Life Sciences, Peking University, Beijing 100871, China

[4]School of Life Sciences, Tsinghua University, Beijing 100084, China

[5]Co-first author

*Correspondence: sun_yujie@pku.edu.cn (Y.S.), liyulab@mail.tsinghua.edu.cn (L.Y.)

http://dx.doi.org/10.1016/j.devcel.2016.04.014

SUMMARY

Autophagic lysosome reformation (ALR) plays an important role in maintaining lysosome homeostasis. During ALR, lysosomes are reformed by recycling lysosomal components from autolysosomes. The most noticeable step of ALR is autolysosome tubulation, but it is currently unknown how the process is regulated. Here, using an approach combining in vivo studies and in vitro reconstitution, we found that the kinesin motor protein KIF5B is required for autolysosome tubulation and that KIF5B drives autolysosome tubulation by pulling on the autolysosomal membrane. Furthermore, we show that KIF5B directly interacts with PtdIns(4,5)P_2. Kinesin motors are recruited and clustered on autolysosomes via interaction with PtdIns(4,5)P_2 in a clathrin-dependent manner. Finally, we demonstrate that clathrin promotes formation of PtdIns(4,5)P_2-enriched microdomains, which are required for clustering of KIF5B. Our study reveals a mechanism by which autolysosome tubulation was generated.

INTRODUCTION

Lysosomes are the digestive organelles of cells. Lysosomes can degrade materials taken up from outside the cell as well as intracellular materials. Extracellular materials are delivered to lysosomes through endocytosis or phagocytosis, while intracellular materials are delivered through autophagy (Luzio et al., 2007). Autophagy is an evolutionarily conserved, lysosome-based degradation pathway. Stimuli such as starvation lead to formation of double-membrane autophagosomes (Mizushima, 2007). Multiple lysosomes fuse with an autophagosome to form an autolysosome, where sequestered cellular contents are degraded. At the peak of autophagy activity, the majority of lysosomes are fused with autophagosomes to form autolysosomes, resulting in a dramatically decreased number of free lysosomes (Yu et al., 2010). Since autophagy occurs regularly in most tissues during the feed-fast cycle, there must be a mechanism to restore the level of free lysosomes after induction of autophagy, otherwise lysosome homeostasis cannot be maintained.

Previously, we reported a mechanism to maintain lysosome homeostasis during autophagy. We found that nascent lysosomes can be recycled from autolysosomes through a process we termed autophagic lysosome reformation (ALR) (Yu et al., 2010). During ALR, tubular structures named reformation tubules are extruded from autolysosomes. Reformation tubules eventually pinch off to form small proto-lysosomes. After a maturation process, proto-lysosomes become acidic and acquire degradative capacity, finally emerging as functional lysosomes (Yu et al., 2010).

Our follow-up work found that the lysosomal efflux transporter Spinster is essential for initiating ALR (Rong et al., 2011), and more recently we unveiled the molecular pathway that regulates ALR, in which clathrin and phosphatidylinositol 4,5-bisphosphate (PtdIns(4,5)P_2) are the central components. During ALR, PtdIns(4,5)P_2 is generated on autolysosomes by PIP5K1B, a phosphatidylinositol 4-phosphate (PtdIns4P) kinase. Clathrin is recruited to autolysosomes by PtdIns(4,5)P_2 and is required to form bud-like structures on the surface of autolysosomes. Although the underlying mechanism is not fully understood, these bud-like structures appear to be required for the generation of reformation tubules and for ALR (Rong et al., 2012).

The most noticeable step of ALR is generation of reformation tubules. During this process, LAMP1-positive tubules are extruded from autolysosomes. These tubules are 80–100 nm in diameter and can be as long as 8 μm (Rong et al., 2012). They are highly dynamic, oscillating back and forth after rapid extrusion. Nascent lysosomes have been observed to pinch off from reformation tubules. So far there have been no reports about how reformation tubules are generated.

Kinesins are microtubule-based motor proteins that move along microtubule filaments (Vale et al., 1985). Kinesins were first discovered in giant squid axons (Vale et al., 1985), and more than 14 kinesin families have been identified so far (Miki et al., 2005). Kinesins are required for many vital cellular functions, such as mitosis, meiosis, and transport of a diverse array of cellular cargoes such as protein complexes, vesicles, and organelles (Hirokawa and Noda, 2008). KIF5B, a member of the Kinesin 1

family, is ubiquitously expressed (Tanaka et al., 1998) and has an NH_2-terminal motor domain and a C-terminal cargo-binding domain. KIF5 proteins play essential roles in axonal transport, and lysosome and mitochondria are also transported by KIF5 proteins (Cardoso et al., 2009; Tanaka et al., 1998). KIF proteins bind to their cargo through their cargo-binding domains and adaptor proteins (Hirokawa and Noda, 2008). Various KIF proteins have been shown to directly bind to phospholipids (Klopfenstein et al., 2002; Venkateswarlu et al., 2005), and this KIF/phospholipid binding is required for KIF-mediated cargo transportation. For example, KIF1A has been shown to bind its cargo through interaction between its pleckstrin homology domain and PtdIns(4,5)P_2. This interaction promotes KIF1A clustering on PtdIns(4,5)P_2-enriched membrane surfaces, and is required for fully efficient vesicle transport (Klopfenstein et al., 2002).

Besides transporting vesicles and organelles, KIF proteins have been shown to be able to induce membrane tubulation in vitro (Dabora and Sheetz, 1988; Vale and Hotani, 1988; Wang et al., 2015). When KIFs are mixed with membrane extracts from different sources and Taxol-stabilized microtubules, membrane networks are formed. KIF1 has also been shown to cause the formation of membrane tubes in an in vitro reconstitution system using giant unilamellar vesicles (GUVs), Taxol-stabilized microtubules, and purified KIF protein. In this system, biotinylated KIF1 is linked to biotinylated GUVs by streptavidin-coated beads or molecular streptavidin (Koster et al., 2003; Roux et al., 2002). Collectively, these experiments established that kinesins are able to drive membrane tubule formation and that KIFs may play important roles in forming membrane tubules or membrane networks in vivo.

Here, we report a mechanism by which autolysosome tubulation was generated. We found that knockout of *kif5b* abolishes the generation of reformation tubules, while replacing KIF5B, but not mobility-defective mutant KIF5B, restores autolysosome tubulation. Using purified KIF5B protein, Taxol-stabilized microtubules and purified autolysosomes, we were able to set up an in vitro system in which autolysosome tubulation is recapitulated. This in vitro reconstitution system and its variants enabled us to carry out in-depth mechanistic studies of autolysosome tubulation. We found that PtdIns(4,5)P_2 is required for KIF5B-driven autolysosome tubulation, KIF5B can bind to PtdIns(4,5)P_2, and the interaction between KIF5B and PtdIns(4,5)P_2 is sufficient to drive tubulation of liposomes containing PtdIns(4,5)P_2. Furthermore, we demonstrate that clathrin can promote tubulation of autolysosomes and liposomes containing PtdIns(4,5)P_2 in vitro and that clathrin is capable of causing formation of PtdIns(4,5)P_2-enriched microdomains in assays using synthetic GUVs. We further demonstrate that KIF5B clusters on PtdIns(4,5)P_2-enriched microdomains. Our data imply that clathrin may promote autolysosome tubulation by facilitating KIF5B recruitment and clustering via clathrin-mediated formation of PtdIns(4,5)P_2-enriched microdomains.

RESULTS

Kinesin 1 KIF5B Is Required for ALR

KIF5B has been identified as a tubular autolysosome-associated protein in our previous study (Rong et al., 2012). We tested the role of KIF5B in ALR by knockout of *kif5b* in NRK cells which stably express CFP-LC3 and LAMP1-mCherry(Red). In *kif5b* knockout cells, at 8 hr after starvation reformation tubules are completely absent, while in control cells reformation tubules are formed normally. To further verify the role of KIF5B in autolysosome tubulation, we established a rescue cell line in which we stably expressed TET-ON-KIF5B in *kif5b*$^{-/-}$ cells (Figures 1A and 1B). Western blotting verified that treating this cell line with 0.5 μg/ml tetracycline restored KIF5B expression (Figure 1C). As we expected, autolysosome tubulation was completely restored (Figure 1A). These results indicate that KIF5B is required for autolysosome tubulation. We hypothesized that mobility of KIF5B is required for autolysosome tubulation. To test this, we stably expressed TET-ON-KIF5BT92N, a mutant KIF5B that lacks mobility, in *kif5b*$^{-/-}$ cells. This mutant failed to rescue autolysosome tubulation, indicating that mobility of KIF5B is required for KIF5B-driven autolysosome tubulation (Figures 1D–1F). We also observed the formation of large, LC3/LAMP1-positive autolysosomes and markedly reduced numbers of lysosomes in a majority of *kif5b*$^{-/-}$ cells, which is the characteristic phenotype when ALR is blocked (Rong et al., 2012). The lysosome number is restored in cells expressing wild-type but not mutant KIF5B (Figures 1G and 1H). Next, we examined the localization of KIF5B in NRK cells during starvation-induced autophagy. We found that after 8 hr of starvation, KIF5B is partially co-localized with LAMP1-positive autolysosomes; similarly, in the rescue cell lines, both KIF5B and KIF5B T92N are also partially co-localized with autolysosomes (Figure S1). We also tested other kinesins and found that overexpression of KIF5A and KIF5C, which also belong to the Kinesin 1 family and have a very low expression level in NRK cells, can restore autolysosome tubulation, while overexpression of KIF1A, a member of the Kinesin 3 family, failed to rescue autolysosome tubulation (Figures 1I–1K) (Miki et al., 2005).

KIF5B Drives Tubulation of Purified Autolysosomes In Vitro

We used an in vitro reconstitution system to test whether pulling by KIF5B causes autolysosome tubulation. First, we isolated autolysosomes from NRK cells by double-density gradient centrifugation (Figure 2A) and purified full-length KIF5B using the baculovirus expression system (Figure 2B). The motor activity of full-length KIF5B was checked by a gliding assay (Movie S1). When we incubated full-length KIF5B or glutathione S-transferase (GST) with purified autolysosomes, we found that KIF5B was pulled down by the autolysosomes (Figure 2C). Next, we tested whether the association between full-length KIF5B and purified autolysosomes is able to cause tubulation of autolysosomes in an in vitro system. In this system, full-length KIF5B is first incubated with purified autolysosomes, then the mixture is transferred to a microtubule-coated glass chamber (Figure 2D) and the tubulation triggered by adding ATP. We found that in the presence of ATP, at least 30% of autolysosomes can form tubules, while no tubules were formed without ATP (Figures 2E–2G). Furthermore, these tubules were elongated along microtubules (Figure 2H). Adding Atto488-labeled recombinant KIF5B into the reaction mixtures revealed that KIF5B is present on both the main body and the tubular part of an autolysosome (Figure S2). Immunostaining using a LAMP1 antibody confirmed that these tubular structures are LAMP1 positive and share

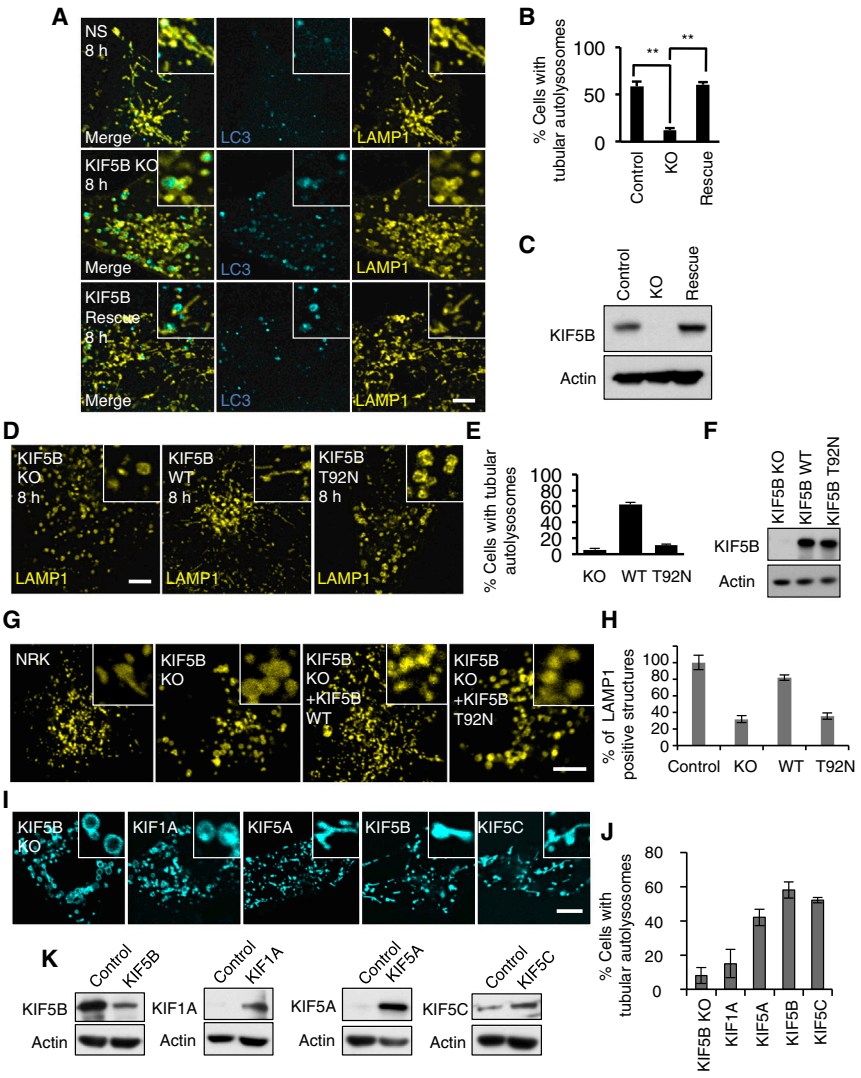

Figure 1. KIF5B Regulates Autolysosome Tubulation

(A) CRISPR/Cas-mediated knockout was used to generate *kif5b*$^{-/-}$ cells. See also Figure S6. Control and *kif5b*$^{-/-}$ NRK cells that stably express TET-ON-KIF5B were transfected with CFP-LC3 and LAMP1-mCherry(Red) plasmids, treated with 0.5 μg/ml tetracycline, and starved for 8 hr. Scale bar, 5 μm.

(B) Cells from (A) were assessed for tubular autolysosomes after starvation and quantified. n = 50 cells from three independent experiments. Error bars indicate the SD. **p < 0.01. See also Figure S1.

(C) The expression of KIF5B from (A) was monitored by western blotting.

(D) *Kif5b*$^{-/-}$ NRK cells that stably express TET-ON-KIF5B or TET-ON-KIF5B T92N were transfected with CFP-LC3 and LAMP1-mCherry(Red) plasmids, treated with 0.5 μg/ml tetracycline, and starved for 8 hr. Scale bar, 5 μm.

(E) Cells from (D) were quantified for tubular autolysosomes. n = 50 cells from three independent experiments. Error bars indicate the SD.

(F) The expression of KIF5B and KIF5BT92N was induced with 0.5 μg/ml tetracycline and monitored by western blotting.

(G) NRK, *kif5b*$^{-/-}$ cells, and *kif5b*$^{-/-}$ cells stably expressing KIF5B WT or KIF5B T92N were transfected with LAMP1-mCherry(Red) plasmids and starved for 12 hr. Scale bar, 5 μm.

(H) Cells from (G) were assessed for the proportion of LAMP1-positive structures after 12 hr of starvation and quantified. All numbers were normalized against values obtained from NRK cells. n > 50 cells from three independent experiments were quantified. Error bars indicate the SD.

(I) KIF1A, KIF5A, KIF5B, or KIF5C were transfected into *kif5b*$^{-/-}$ cells expressing LAMP1-YFP. Cells were starved for 8 hr. Scale bar, 5 μm.

(J) Cells from (I) were assessed for tubular autolysosomes after 8 hr of starvation and quantified. n > 50 cells from three independent experiments were quantified. Error bars indicate the SD.

(K) Protein expression levels were analyzed by western blot using anti-KIF1A, anti-KIF5A, anti-KIF5B, or anti-KIF5C antibodies.

similar morphological features with tubular autolysosomes in vivo (Figure 2I). As a control, we also tested whether KIF5BT92N can cause autolysosome tubulation in vitro. As we expected, although the KIF5B mutant still could bind to autolysosomes (Figure S2), it failed to cause autolysosome tubulation (Figures 2J–2L). These data suggest that we have indeed reconstituted autolysosome tubulation in vitro, and that KIF5B regulates ALR by pulling the reformation tubules from autolysosomes.

KIF5B Interacts with PtdIns(4,5)P_2, and the KIF5B-PtdIns(4,5)P_2 Interaction Is Sufficient to Drive Liposome Tubulation

Previously we reported the presence of PtdIns(4,5)P_2 on autolysosomes and showed that PIP5K1B, the kinase that converts PtdIns4P into PtdIns(4,5)P_2, is required for ALR, as knockdown of *pip5k1b* totally blocks autolysosome tubulation in vivo (Rong et al., 2012). We found that purified autolysosomes from *pip5k1b* knockdown cells cannot be tubulated in the in vitro reconstitution system (Figures 3A and 3B). In contrast, knockdown of *klc1* and *klc2*, the known KIF5B adaptors that are expressed in NRK cells, has no effect on autolysosome tubulation (Figure S3), indicating that KIF5B may regulate autolysosome tubulation via PtdIns(4,5)P_2.

Next, we tested whether KIF5B can bind to PtdIns(4,5)P_2. A lipid overlay assay indicated that KIF5B can bind to PtdIns4P, PtdIns(4,5)P_2 and phosphatidylinositol 3,4,5-trisphosphate (Figure S4). To further confirm the interaction between PtdIns(4,5)P_2 and KIF5B, we prepared liposomes with 10% PtdIns(4,5)P_2, and used a sedimentation assay to show that these liposomes were able to bind KIF5B but not GST (Figure 3C). We then varied the amount of PtdIns(4,5)P_2 in the liposomes and found that at least10% PtdIns(4,5)P_2 is required for liposome-KIF5B binding to be detected by the sedimentation assay (Figure 3D). Domain mapping using flotation assay revealed that amino acids 814–963 of the cargo domain are responsible for the interaction between KIF5B and PtdIns(4,5)P_2 (Figure S5).

To test whether the binding between PtdIns(4,5)P_2 and KIF5B is sufficient to drive liposome tubulation, we incubated

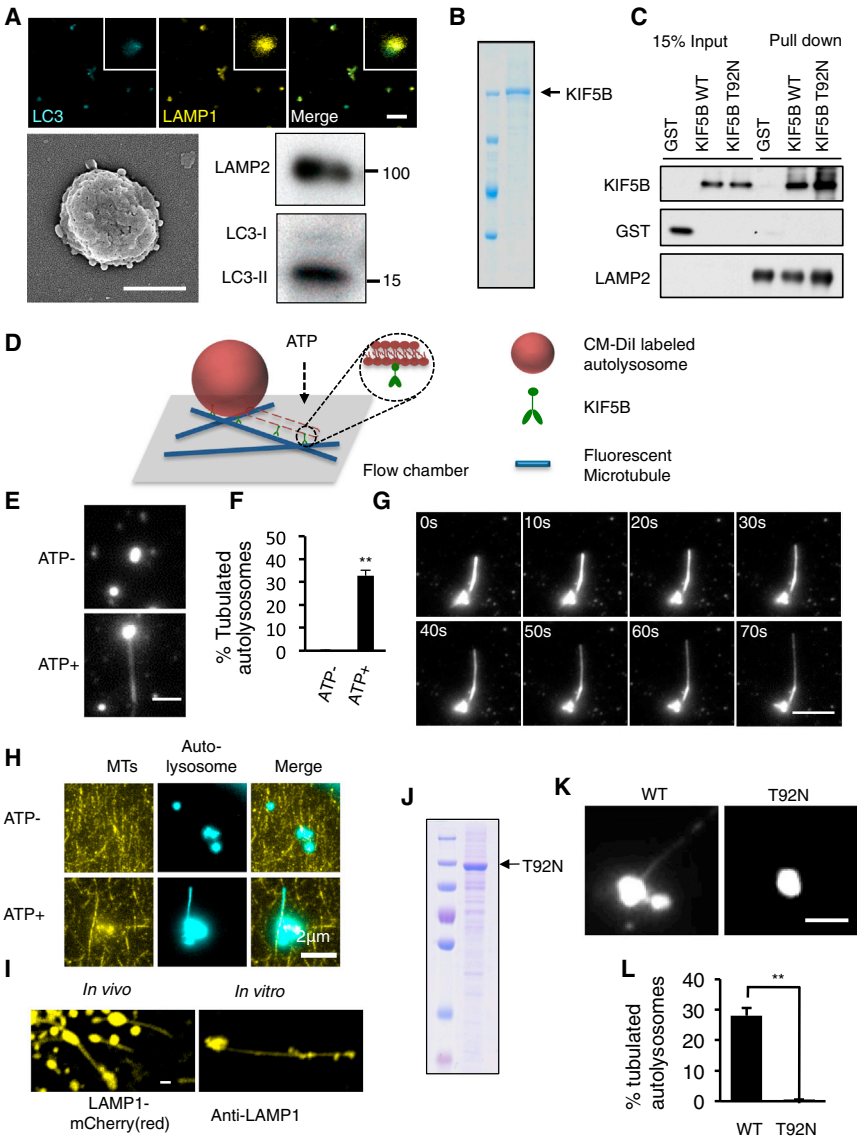

Figure 2. KIF5B Drives Autolysosome Tubulation In Vitro

(A) Autolysosomes were purified from NRK cells and stained with antibodies against LAMP1 and LC3 (top). Scale bar, 1 μm. The quality of purified autolysosomes was monitored by scanning electron microscopy (bottom left). Scale bar, 500 nm. Purified autolysosomes were analyzed by western blot using anti-LAMP2 and anti-LC3 antibodies (bottom right).

(B) Full-length KIF5B was expressed using the Bac-to-Bac expression system, and the purity of KIF5B was analyzed by Coomassie staining. The motor activity of full-length KIF5B was checked by a gliding assay shown in Movie S1.

(C) Purified autolysosomes were incubated with full-length KIF5B or KIF5B T92N, washed, and analyzed by western blotting with antibodies against His-tag, GST, and LAMP2.

(D) Schematic diagram of in vitro autolysosome tubulation. Purified autolysosomes were incubated with full-length KIF5B on ice, transferred into flow chamber channels, and visualized in the presence of ATP.

(E) Purified autolysosomes were labeled by CM-DiI, incubated with KIF5B, and transferred into flow chamber channels. The images were collected with a Nikon TIRF microscope. Scale bar, 2 μm.

(F) The percentage of tubulated autolysosomes was determined from (E). n > 100 from three independent experiments. Error bars indicate the SD. **p < 0.01.

(G) Time-lapse sequence of autolysosome tubulation in the presence of ATP. Scale bar, 2 μm.

(H) Purified autolysosomes were stained by CM-DiI (cyan), incubated with full-length KIF5B, and transferred into flow chamber channels coated with Hilyte Fluor 647-labeled microtubules (yellow). The images were collected with a Nikon TIRF microscope. Scale bar, 2 μm. See also Figure S2.

(I) Left: NRK cells stably expressing CFP-LC3 and LAMP1-mCherry(Red) were starved for 8 hr, and reformation tubules were visualized by confocal microscopy. Scale bar, 1 μm. Right: samples from (E) were stained with antibody against LAMP1, and observed by confocal microscopy. Scale bar, 1 μm.

(J) Full-length KIF5B T92N was expressed using the Bac-to-Bac expression system, and the purity of KIF5B T92N was analyzed by Coomassie staining.

(K) Purified autolysosomes were labeled by CM-DiI, incubated with KIF5B, and transferred into flow chamber channels. The images were collected with a Nikon TIRF microscope. Scale bar, 2 μm. See also Figure S2.

(L) The percentage of tubulated autolysosomes was determined from (K). n > 100 from three independent experiments. Error bars indicate the SD. **p < 0.01.

full-length KIF5B with liposomes containing various concentrations of PtdIns(4,5)P_2, transferred the mixture to microtubule-coated glass chambers, then triggered tubulation by adding ATP. No liposomes containing 0% PtdIns(4,5)P_2 were observed at the illumination depth of the total internal reflection fluorescence (TIRF) microscope, indicating that these liposomes cannot bind to KIF5B. In contrast, liposomes containing 5% PtdIns(4,5)P_2 were observed at the illumination depth. However, after adding ATP, there was very little liposome tubulation under these conditions. Tubulation became evident in liposomes containing 10% PtdIns(4,5)P_2, and the efficiency of tubulation increased in a PtdIns(4,5)P_2 concentration-dependent manner (Figures 3E–3G). Taking all these data together, we conclude that PtdIns(4,5)P_2 is required for autolysosome tubulation, and the interaction between KIF5B and PtdIns(4,5)P_2 is sufficient to drive the tubulation of PtdIns(4,5)P_2-containing liposomes.

Clathrin Is Required for KIF5B-Driven Autolysosome Tubulation

The physiological level of PtdIns(4,5)P_2 in membranes is relatively low, with 5% considered the upper limit of local concentrations. The fact that 5% PtdIns(4,5)P_2 is not sufficient to drive the in vitro tubulation of liposomes indicated that the binding between PtdIns(4,5)P_2 and KIF5B alone may not be enough to cause tubulation under physiological conditions.

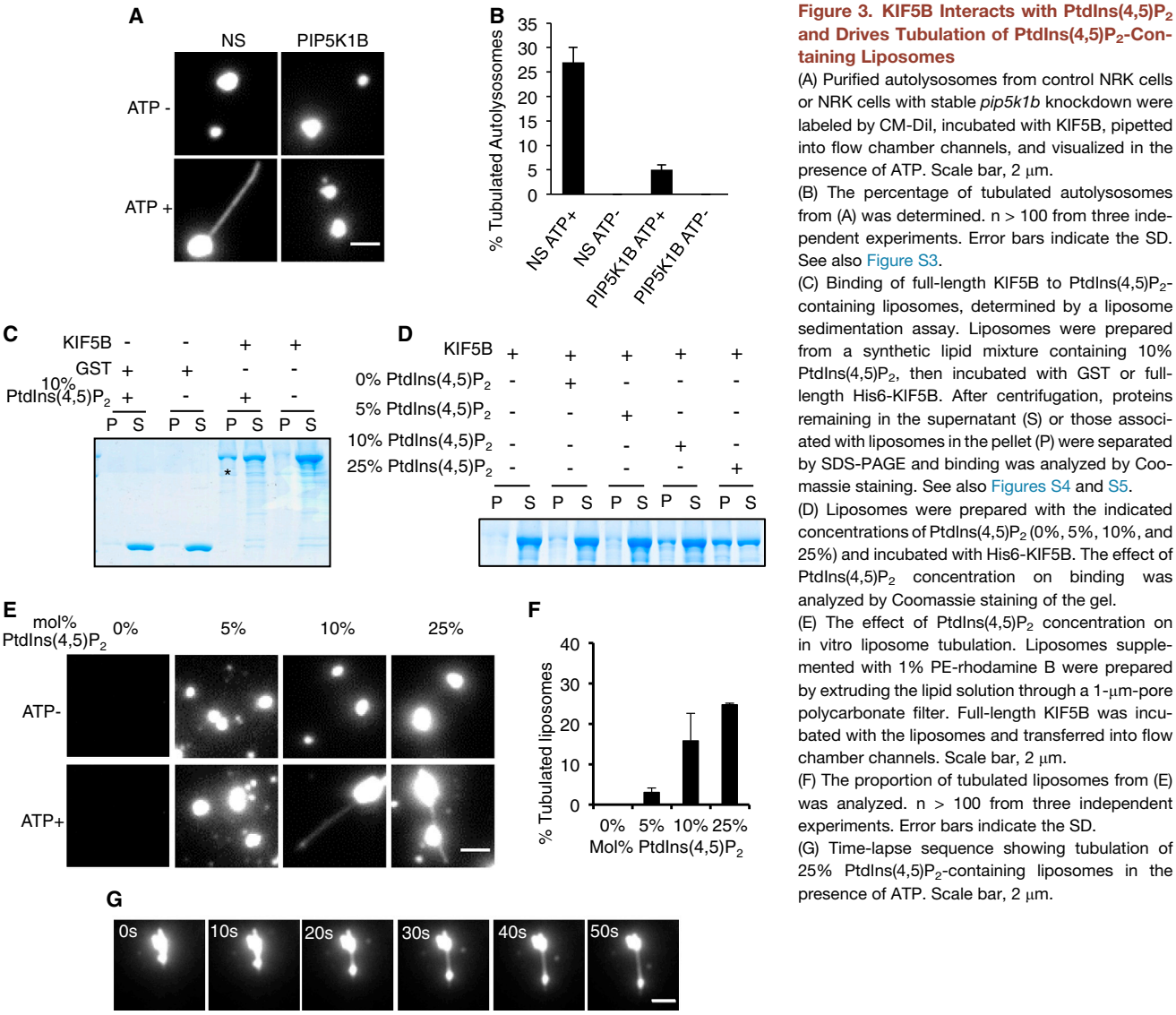

Figure 3. KIF5B Interacts with PtdIns(4,5)P_2 and Drives Tubulation of PtdIns(4,5)P_2-Containing Liposomes

(A) Purified autolysosomes from control NRK cells or NRK cells with stable *pip5k1b* knockdown were labeled by CM-DiI, incubated with KIF5B, pipetted into flow chamber channels, and visualized in the presence of ATP. Scale bar, 2 μm.

(B) The percentage of tubulated autolysosomes from (A) was determined. n > 100 from three independent experiments. Error bars indicate the SD. See also Figure S3.

(C) Binding of full-length KIF5B to PtdIns(4,5)P_2-containing liposomes, determined by a liposome sedimentation assay. Liposomes were prepared from a synthetic lipid mixture containing 10% PtdIns(4,5)P_2, then incubated with GST or full-length His6-KIF5B. After centrifugation, proteins remaining in the supernatant (S) or those associated with liposomes in the pellet (P) were separated by SDS-PAGE and binding was analyzed by Coomassie staining. See also Figures S4 and S5.

(D) Liposomes were prepared with the indicated concentrations of PtdIns(4,5)P_2 (0%, 5%, 10%, and 25%) and incubated with His6-KIF5B. The effect of PtdIns(4,5)P_2 concentration on binding was analyzed by Coomassie staining of the gel.

(E) The effect of PtdIns(4,5)P_2 concentration on in vitro liposome tubulation. Liposomes supplemented with 1% PE-rhodamine B were prepared by extruding the lipid solution through a 1-μm-pore polycarbonate filter. Full-length KIF5B was incubated with the liposomes and transferred into flow chamber channels. Scale bar, 2 μm.

(F) The proportion of tubulated liposomes from (E) was analyzed. n > 100 from three independent experiments. Error bars indicate the SD.

(G) Time-lapse sequence showing tubulation of 25% PtdIns(4,5)P_2-containing liposomes in the presence of ATP. Scale bar, 2 μm.

Previously we showed that clathrin is required for tubulation of autolysosomes, as there are no visible reformation tubules in *clathrin* knockdown cells (Rong et al., 2012). This observation prompted us to test whether clathrin can facilitate KIF5B-driven autolysosome tubulation. In our previous study, we found that clathrin and PtdIns(4,5)P_2 are located on bud-like structures on the surface of autolysosomes. Clathrin can be stripped from autolysosomes by treating purified autolysosomes with trypsin. Incubating these "stripped" autolysosomes with rat brain cytosol and an ATP regeneration system caused recruitment of clathrin to the autolysosomes and reconstituted the buds. Adding clathrin antibody potently blocked the formation of buds (Rong et al., 2012). Based on this reconstitution protocol, we developed a double reconstitution protocol to test the role of clathrin in KIF5B-driven autolysosome tubulation (Figure 4A). First, we incubated stripped autolysosomes or liposomes containing 5% PtdIns(4,5)P_2 with rat brain cytosol and an ATP regeneration system to reconstitute the clathrin buds, then added these reconstituted autolysosomes or liposomes to our in vitro tubulation system. Using this approach, we found that KIF5B cannot drive tubulation of stripped autolysosomes; however, tubulation of stripped autolysosomes can be restored by reconstituting clathrin buds (Figures 4B and 4C). Addition of a clathrin antibody totally abolishes tubulation in this system (Figures 4D and 4E). Similarly, reconstituting clathrin on liposomes containing 5% PtdIns(4,5)P_2 can promote KIF5B-driven tubulation (Figures 4F and 4G), and the tubulation is blocked by adding clathrin antibody during the first step (Figures 4H and 4I). These data imply that KIF5B and clathrin may coordinately drive the tubulation of autolysosomes.

Clathrin Promotes Formation of PtdIns(4,5)P_2-Enriched Microdomains

Previously we have shown that PtdIns(4,5)P_2 is enriched on microdomains on the surface of autolysosomes (Rong et al., 2012). We wondered whether the recruitment of clathrin can promote the formation of PtdIns(4,5)P_2-enriched-microdomains. To test this idea, we generated GUVs containing Top Fluor-labeled

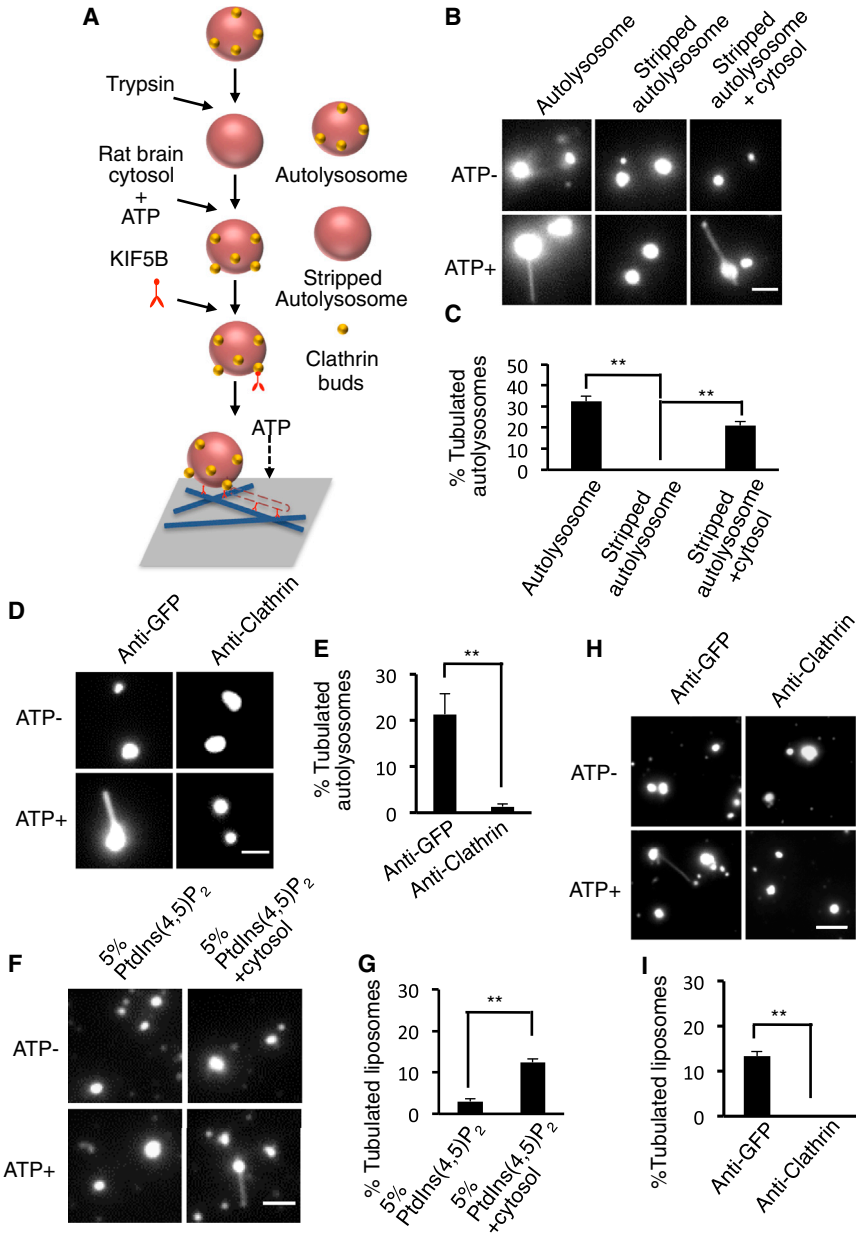

Figure 4. Clathrin Facilitates Tubulation of Autolysosomes and PtdIns(4,5)P_2-Containing Liposomes

(A) Schematic diagram of the double in vitro tubulation system. Stripped autolysosomes, prepared by treating autolysosomes with trypsin, were first incubated with rat brain cytosol and an ATP regeneration system, then the reconstituted autolysosomes were washed and incubated with KIF5B and pipetted into flow chamber channels. ATP was added to trigger tubulation, which was observed with a TIRF microscope.

(B) Autolysosomes, stripped autolysosomes, and reconstituted autolysosomes were labeled by CM-DiI, incubated with KIF5B, and transferred into flow chamber channels. Tubulation was triggered by adding ATP and the reaction was observed with a TIRF microscope. Scale bar, 2 μm.

(C) The percentage of tubulated autolysosomes from (B) was determined. n > 100 from three independent experiments. Error bars indicate the SD. **p < 0.01.

(D) Stripped autolysosomes were incubated with rat brain cytosol pre-treated with antibodies against GFP or clathrin heavy chain. Reconstituted autolysosomes were incubated with KIF5B and the mixture was then pipetted into flow chamber channels. Tubulation was triggered by adding ATP and the reaction was observed with a TIRF microscope. Scale bar, 2 μm.

(E) The percentage of tubulated autolysosomes from (D) was determined. n > 100 from three independent experiments. Error bars indicate the SD. **p < 0.01.

(F) Liposomes containing 5% PtdIns(4,5)P_2 were first incubated with rat brain cytosol and an ATP regeneration system, then washed, incubated with KIF5B, and pipetted into flow chamber channels. Tubulation was triggered by adding ATP and the reaction was observed by TIRF microscopy. Scale bar, 2 μm.

(G) The percentage of tubulated liposomes from (F) was analyzed. n > 100 from three independent experiments. Error bars indicate the SD. **p < 0.01.

(H) Liposomes containing 5% PtdIns(4,5)P_2 were incubated with rat brain cytosol pre-treated with antibodies against GFP and clathrin heavy chain. The mixture was then incubated with KIF5B and transferred into flow chamber channels. Tubulation was triggered by adding ATP and the reaction was observed by TIRF microscopy. Scale bar, 2 μm.

(I) The percentage of tubulated liposomes from (H) was determined. n > 100 from three independent experiments. Error bars indicate the SD. **p < 0.01.

PtdIns(4,5)P_2. Under control conditions, PtdIns(4,5)P_2 is evenly distributed on GUVs; however, when the vesicles were incubated with rat brain cytosol in the presence of an ATP regeneration system, PtdIns(4,5)P_2 formed microdomains on the GUVs. Adding clathrin antibody, but not a control antibody, to the rat brain cytosol markedly blocked the formation of PtdIns(4,5)P_2 microdomains (Figures 5A and 5B).

Next, we tested whether the PtdIns(4,5)P_2 microdomains can recruit KIF5B. We added Atto550-labeled recombinant KIF5B to the reaction and found that KIF5B was evenly distributed on the PtdIns(4,5)P_2-containing GUVs; however, when the PtdIns(4,5)P_2 microdomains were reconstituted, KIF5B was highly enriched on PtdIns(4,5)P_2 microdomains (Figures 5C and 5D), but not on the rest of the GUVs. These data imply that clathrin-mediated formation of PtdIns(4,5)P_2-enriched microdomains may be required for clustering of KIF5B on autolysosomes.

To test this hypothesis, we examined the localization of KIF5B in NRK cells during starvation-induced autophagy. We found that after 4 hr of starvation, KIF5B clusters on LAMP1-positive autolysosomes; however, in *clathrin* or *pip5k1b* knockdown cells, clustering of KIF5B on autolysosomes during starvation is markedly impaired (Figures 5E–5J). We also found that starvation markedly enhanced the co-localization of clathrin with KIF5B (Figures 5K

and 5L). These data suggest that clathrin and PtdIns(4,5)P_2 are required for recruitment of KIF5B to autolysosomes, and that clathrin may facilitate the recruitment of KIF5B by promoting the formation of PtdIns(4,5)P_2-enriched microdomains.

DISCUSSION

In this work, we demonstrated that KIF5B can drive autolysosome tubulation by pulling. Previous studies have suggested that kinesins are responsible for several membrane deformation processes. It makes sense intuitively that kinesins, as molecular motors, can apply the force necessary for tubulation, but the mechanisms that regulate this process are poorly understood. In this work, we discovered that locally concentrated kinesin motors, enriched in microdomains, are essential for ALR. Specifically, we demonstrated that clathrin can promote the formation of PtdIns(4,5)P_2-enriched microdomains on autolysosomes, which then cause clustering of KIF5B. These "KIF5B clusters" may serve as sites to initiate tubulation, owing to the high local concentration of KIF5B in these clusters (Figure 6). It is worth noting that although KIF5B is required for autolysosome tubulation in vivo and KIF5B is sufficient to cause autolysosome tubulation in vitro, we cannot rule out the possibility that KIF5B is involved only in the initiation step with other kinesins mediating the elongation step.

Clathrin plays important roles in various biological processes including endocytosis, congression of chromosomes, and ALR (McMahon and Boucrot, 2011; Mousavi et al., 2004; Rong et al., 2012; Royle et al., 2005). The role of clathrin in endocytosis is very well established, and the current view of the function of clathrin in other cellular processes is largely derived from studies of endocytosis, in which clathrin facilitates the budding of endocytic vesicles by forming a clathrin coat. However, this mechanism does not fully explain the role of clathrin in some clathrin-dependent biological processes. During endocytosis, clathrin is recruited to the plasma membrane by adaptor protein 2 (AP2) through the direct interaction between PtdIns(4,5)P_2 and AP2 (Honing et al., 2005). A typical clathrin lattice contains 108 clathrin units. Every clathrin interacts with two AP2 molecules, and every AP2 can interact with two PtdIns(4,5)P_2; thus, a typical clathrin lattice could contain 432 PtdIns(4,5)P_2 molecules. Formation of clathrin lattices may therefore serve as a mechanism to enrich PtdIns(4,5)P_2. Since PtdIns(4,5)P_2 is known to interact with many other molecules, the theoretical enrichment of PtdIns(4,5)P_2 by clathrin, if proved to be true, may be another mechanism for the regulation of biological processes (Collins et al., 2002; Mousavi et al., 2004).

The formation of microdomains may play at least two roles in ALR. Previous studies on GUVs have shown that initiation of tubulation needs to overcome a large energy barrier, and consequently kinesin must be locally concentrated on the vesicle (Campas et al., 2008; Leduc et al., 2004). Thus, a group of kinesin motors may concentrate in a microdomain to perform work that is not possible for individual motors. In addition, the assembly of clathrin at the microdomain drives formation of buds, which increases the local curvature and thus reduces the energy barrier to initiate membrane deformation. Our data reveal an unexpected role of clathrin in promoting motor protein-driven membrane tubulation, which may be relevant to other clathrin-mediated cellular processes.

EXPERIMENTAL PROCEDURES

Reagents and Materials

All lipids (brain polar lipids [141101], phosphatidylcholine [850457C], phosphatidylethanolamine [PE; 850725C], PtdIns(4,5)P_2 [840046X], and PE-rhodamine B [810158P]) were purchased from Avanti Polar Lipids. All other chemicals were purchased from Sigma-Aldrich except guanosine triphosphate (GTP) and Taxol, which were purchased from Cytoskeleton. Anti-LAMP1 (L1418) antibody was from Sigma-Aldrich. Anti-LAMP2 (EP-6041) antibody was from MBL. Anti-GFP (11814460001) antibody and anti-His_6 (11922416001) antibody were from Roche. Anti-clathrin heavy-chain (2410) antibody was from Cell Signaling Technology. Anti-PtdIns(4,5)P_2 (Z-G045) antibody was from Echelon Biosciences. Antibodies against GST (ab19256), tubulin, KIF1A (ab180153), KIF5A (ab5628), KIF5B (ab5629), and KIF5C (ab5630) were from Abcam. HTS tubulin (HTS03-A), GTP (BST06-001), and Taxol (TXD01) were obtained from Cytoskeleton.

Cell Culture and Transfection

NRK cells were obtained from the American Type Culture Collection and cultured in DMEM medium (Life Technologies) supplemented with 10% fetal bovine serum (FBS) (5% CO_2). Cells were transfected with 200 pmol of RNAi or a total of 2 μg of DNA through Amaxa nucleofection using solution T and program X-001. Cells were then cultured in growth medium for further analysis.

Generation of NRK Cells with Stable Knockout of *kif5b* and Tetracycline-Inducible Expression of KIF5B

The CRISPR/Cas9 system was adapted to generate NRK cells with stable knockout of *kif5b* (Multiplex Genome Engineering Using CRISPR/Cas Systems). The single guide RNA-binding sequence (5′-GTAAACTTCATGATC CAGA-3′) was synthesized for KIF5B disruption, then NRK cells were simultaneously transfected with Cas9, guide RNA, and puromycin plasmids. Puromycin screening was used to detect cells with knockout of *kif5b*. Single clones of the cells were picked up and the knockout efficiency of *kif5b* was verified by western blotting. The single clone *kif5b*$^{-/-}$ cells were then tested for DNA-sequencing analysis of mutated alleles in the rat *kif5b* locus (Figure S6A). The off-target recombinations were excluded using T7E1 endonuclease digest assay (Zhou et al., 2014) (Figure S6B).

TET-ON-KIF5B cell lines were generated with the T-REXTM system (K1020-01; Life Technologies). *Kif5b*$^{-/-}$ cells were transfected with pcDNATM6/TR plasmid and a KIF5B-inducible expression construct at the ratio of 6:1 (w/w). Blasticidin and zeocin were used to select TET-ON-KIF5B cells.

Autolysosome Purification

Autolysosome purification was performed according to a lysosome isolation kit (LYSISO1; Sigma-Aldrich) according to the manufacturer's manual and our previous publication (Rong et al., 2012). In brief, about 1 × 10^8 NRK cells were starved for 4 hr in serum-free DMEM medium. Cells were harvested and lysed by Dounce homogenizer. The lysed cells were centrifuged for 10 min at 1,000 × *g*. The supernatant was centrifuged for 20 min at 20,000 × *g*. The pellet was resuspended in 19% Optiprep solution and subjected to the first Optiprep gradient composed of 27%, 22.5%, 19%, 16%, 12%, and 8%. After centrifugation at 150,000 × *g* for 4 hr, the autolysosomes from the first Optiprep gradient centrifugation (the top 1.5 ml) were collected, diluted in PBS, and centrifuged at 20,000 × *g*. The pellet was diluted with 19% Optiprep density gradient medium solution, and overlaid with 22.5%, 19%, 16%, 12%, 8%, 5%, and 3% Optiprep solutions. After centrifugation at 150,000 × *g* for 4 hr, the fractions were collected and analyzed by western blotting and transmission electron microscopy. The purified autolysosomes (top third to fifth fraction, 500 μl/fraction) were collected and used for the in vitro assays. All procedures were conducted at 4°C.

Live-Cell Imaging

Transfected cells were replated in Lab-Tek chambered coverglasses before imaging, and cells were maintained at 37°C with 5% CO_2. Images were acquired using an Olympus FV-1000 confocal microscope.

Immunofluorescence Staining of Cells

Cells were grown on coverslips in 24-well plates. The cells were washed in PBS, fixed in 4% paraformaldehyde for 10 min at room temperature, and

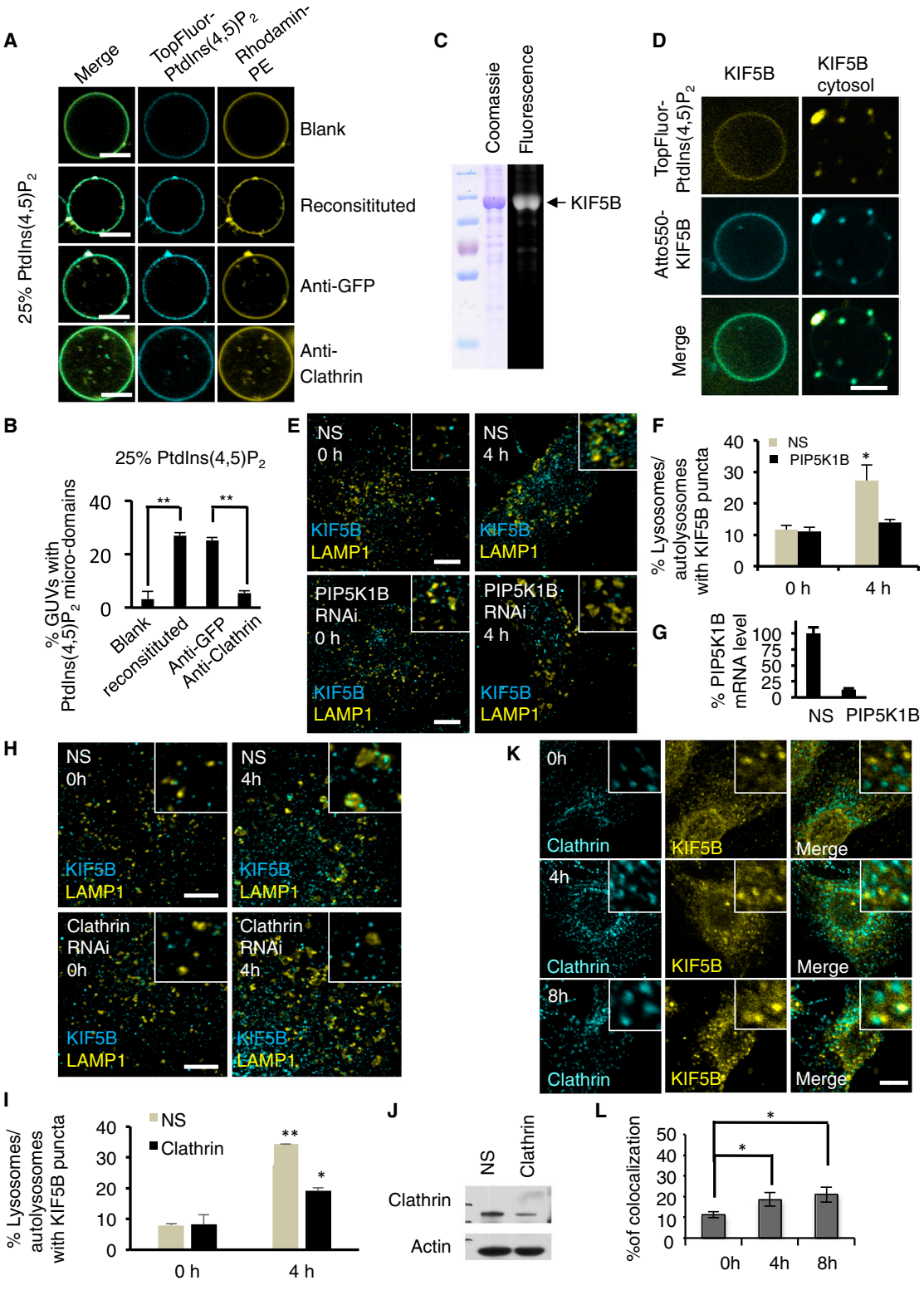

Figure 5. Clathrin Promotes Formation of PtdIns(4,5)P_2-Enriched Microdomains

(A) GUVs containing TopFluor-labeled PtdIns(4,5)P_2 and rhodamine-labeled PE were made by the electroformation method, then incubated with rat brain cytosol pre-treated with antibodies against GFP and clathrin heavy chain for 1 hr. Scale bar, 5 μm.

(B) Quantification of the number of GUVs containing PtdIns(4,5)P_2 microdomains from (A). n > 50 from three independent experiments. Error bars indicate the SD. **p < 0.01.

(legend continued on next page)

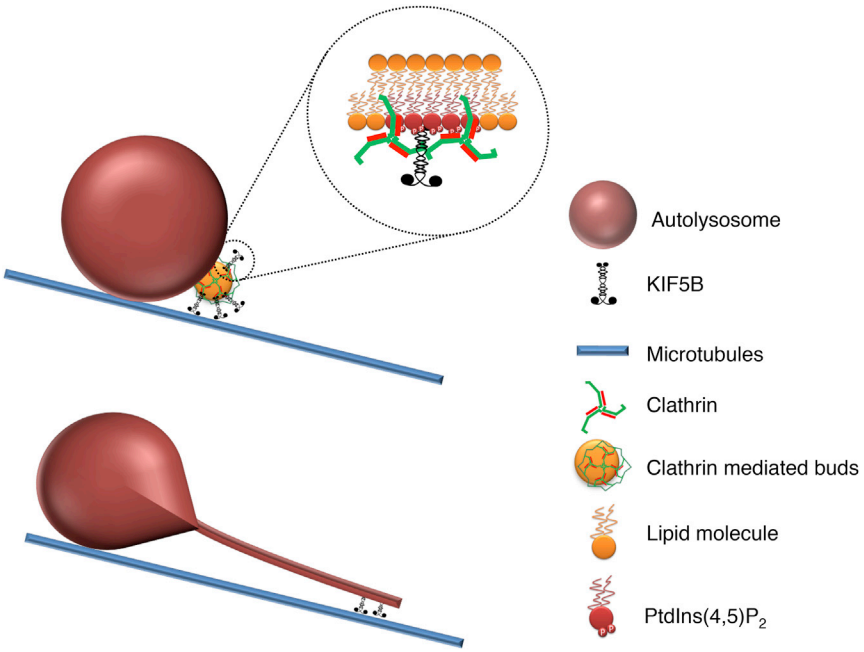

Figure 6. Schematic Illustration of the Role of Clathrin, PtdIns(4,5)P_2, and KIF5B in Autolysosome Tubulation

Clathrin promotes formation of PtdIns(4,5)P_2-enriched microdomains on the surface of autolysosomes. PtdIns(4,5)P_2 recruits KIF5B, which drives autolysosome tubulation.

permeabilized in 0.1% saponin for 30 min. Fixed cells were blocked with 10% FBS in PBS for 30 min, stained with 10 μg/ml antibody in blocking buffer for 1 hr, and washed with PBS. Cells were then stained with secondary antibody in blocking buffer for 1 hr and washed with PBS three times.

In Vitro Immunofluorescence Staining

Autolysosomes were imaged by first allowing them to flow into motility assay chambers and incubate for 20 min to allow them to attach, then the chambers were washed to exclude the unattached autolysosomes and fixed in 4% paraformaldehyde. The sample was then stained with first and secondary antibodies using the immunofluorescence staining protocol. The samples of tubular structures in the in vitro system were directly fixed in 4% paraformaldehyde and stained using the immunofluorescence staining protocol.

Semi-Intact Cell Treatment

KIF5B staining was performed in semi-intact NRK cells. Semi-intact NRK cells were prepared as described previously (Kano et al., 2000) with minor modifications. In brief, NRK cells were grown on coverslips, washed twice with ice-cold PBS, and treated with buffer containing 25 μg/ml digitonin, 25 mM HEPES-KOH (pH 7.2), 125 mM potassium acetate, 5 mM magnesium acetate, 1 mg/ml D-glucose, and 1 mM DTT for 5 min at 4°C, then washed with buffer without digitonin and incubated with buffer without digitonin for 20 min on ice. The cells were then fixed with 4% paraformaldehyde for 10 min at room temperature and subjected to immunofluorescence staining.

Giant Unilamellar Vesicle Preparation and Imaging

GUVs were formed from phosphatidylcholine (50%), phosphatidylethanolamine (25%), PtdIns(4,5)P_2 (25%), TopFluor-labeled PtdIns(4,5)P_2, and/or rhodamine B-labeled phosphatidylethanolamine. GUVs were prepared as described previously (Kaufmann et al., 2014). In brief, a thin, homogeneous lipid film was prepared on OTI-covered glass slides and dried for 30 min then placed in the "vesicle prep pro" machine, and electroformation was carried out at 0.24 V and 9.9 Hz for 90 min at 37°C. The GUVs were harvested after cooling down to room temperature and used immediately. For detection of the distribution of PtdIns(4,5)P_2, GUVs were incubated with rat brain cytosol pre-treated with anti-GFP (400 μg/ml) or anti-clathrin heavy-chain (400 μg/ml) antibodies as indicated at 4°C for 1.5 hr, and an ATP regeneration system. The mixtures were incubated for 1 hr at 38°C. For detection of the location of KIF5B on GUVs, GUVs were incubated with rat brain cytosol, an ATP regeneration system, and Atto550-labeled KIF5B for 30 min. The mixture was incubated for 60 min. Images were acquired using an Olympus FV-1000 confocal microscope.

KIF5B Purification and Labeling

For full-length KIF5B, proteins were expressed by using the Bac-to-Bac expression system (Friedman and Vale, 1999). In brief, Sf9 cells were grown in Lonza medium to a density of ~2 × 10^6 cells/ml and incubated with virus containing full-length KIF5B construct. After 60 hr, cells were collected, lysed by freeze-thaw cycles, and centrifuged at 4°C. The soluble fraction was bound in batches to Ni-nitrilotriacetic acid (NTA) agarose, and the resin was washed. His6-tagged KIF5B was eluted with 20 mM Tris, 0.1 M NaCl, and 250 mM imidazole (pH 8). The eluate was concentrated and stored in 50 μM HEPES-KOH (pH 7.4), 300 mM NaCl, 1 mM $MgCl_2$, 10% (w/v) sucrose, and 50 μM ATP.

(C) Atto550-labeled KIF5B was analyzed on SDS-PAGE gel and Coomassie staining, and the fluorescent label of Atto550-KIF5B was shown by scanning under excitation light at 532 nm.
(D) GUVs containing TopFluor-labeled PtdIns(4,5)P_2 (5%) were incubated with Atto550-labeled KIF5B which is labeled as described in (C), or Atto550-labeled KIF5B with rat brain cytosol and an ATP regeneration system for 1 hr and visualized by confocal microscopy. Scale bar, 5 μm.
(E) NRK cells were transfected with nonspecific (NS)- or *pip5k1b*-RNAi, starved for 0 and 4 hr, treated with 25 μg/ml digitonin, and stained with antibodies against KIF5B and LAMP1. Scale bar, 5 μm.
(F) Autolysosomes from (E) were assessed for the presence of KIF5B puncta and quantified. n > 500 autolysosomes from three independent experiments. Error bars indicate the SD. *p < 0.05 (t test).
(G) The knockdown efficiency of *pip5k1b* was tested by qPCR. Error bars indicate the SD.
(H) NRK cells were transfected with nonspecific (NS)- or *clathrin*-RNAi, starved for 0 and 4 hr, treated with 25 μg/ml digitonin, and stained with antibodies against KIF5B and LAMP1. Scale bar, 5 μm.
(I) The autolysosomes from (H) were assessed for the presence of KIF5B puncta and quantified. n > 500 autolysosomes from three independent experiments. Error bars indicate the SD. *p < 0.05, **p < 0.01 (t test).
(J) The knockdown efficiency of *clathrin* was shown by western blot using anti-clathrin antibody.
(K) NRK cells stably expressing clathrin-GFP were starved for 0, 4, or 8 hr. The cells were then treated with 25 μg/ml digitonin and stained with antibodies against KIF5B and GFP. Scale bar, 10 μm.
(L) Cells from (H) were assessed for co-localization of clathrin and KIF5B. n > 1,000 autolysosomes from three independent experiments were quantified. Error bars indicate the SD.*p < 0.05 (t test).

KIF5B was labeled with Atto550, a monofunctional NHS ester that labels free amino groups, for 30 min on ice. KIF5B-Atto550 was removed from free dye by gel filtration using a NAP5 column.

His-Tag/GST-Tag Protein Purification

Plasmid constructs were expressed in *Escherichia coli* BL21 at 16°C overnight after induction with 0.2 mM isopropyl-β-dithiogalactopyranoside. Tagged proteins were purified from the soluble fraction of the bacterial lysate using either GE Healthcare's Glutathione Sepharose 4B slurry for GST-tagged proteins or Ni-NTA for 6× His-tagged proteins. The glutathione Sepharose was pre-equilibrated in binding buffer (50 mM Tris-HCl [pH 7.5], 150 mM NaCl). Binding of the GST-tagged proteins was performed at 4°C for 2 hr. Protein-bound beads were washed with washing buffer (20 mM Tris-HCl [pH 7.5], 500 mM NaCl) and eluted with 50 mM Tris-HCl (pH 8) and 10 mM reduced glutathione (GE Healthcare). Tagged protein eluted from the beads was exchanged to binding buffer and stored in multiple aliquots at −80°C. For purification of His-tagged proteins, the Ni Sepharose 6 Fast Flow (GE Healthcare 17-5318-06) was pre-equilibrated in binding buffer (50 mM Tris-HCl [pH 7.5], 150 mM NaCl, 10 mM imidazole). His-tagged proteins were allowed to bind to the resin for 2 hr at 4°C. The resin was then washed with washing buffer (20 mM Tris-HCl [pH 7.5], 500 mM NaCl, 30 mM imidazole) and bound proteins were eluted in elution buffer (50 mM Tris-HCl [pH 7.5], 150 mM NaCl, 300 mM imidazole). His-tagged proteins were exchanged to storage buffer (50 mM Tris-HCl [pH 7.5], 150 mM NaCl) and stored in multiple aliquots at −80°C. The protein concentration was determined by Bradford or bicinchoninic acid assay.

Gliding Assays

The gliding assay chambers were prepared as for the motility assay using hydrophilic coverslips. 15-μl full-length KIF5B were incubated in flow chamber channels for 5 min. The kinesin-coated coverslips were blocked with 3 mg/ml casein for 5 min, then 40 nM HyLite647-labeled microtubules was introduced into the flow chamber. An ATP solution containing 0.5 mM ATP, 20 μM Taxol, 10 mM DTT, 1 mg/ml casein, an ATP regeneration system, and an oxygen scavenger system were subsequently added to the chamber. Images were recorded every 0.5 s for 5 min using a Nikon Ti-E TIRF microscope under 640 nm laser excitation. The mean motility velocity was determined from measurements of 20 or more gliding microtubules.

Sedimentation Assay

Liposomes were prepared by dissolving a lipid mixture consisting of phosphatidylcholine, phosphatidylethanolamine, and PtdIns(4,5)P_2 in chloroform followed by evaporation under a constant nitrogen stream. The lipids were rehydrated, and extruded through a 400-nm pore polycarbonate filter using miniextruders from Avanti Polar Lipids. 7-μg proteins were incubated with these liposomes in 20 μl of liposome binding buffer (30 mM Tris-HCl [pH 8.0], 4 mM EGTA, 1 mM DTT, 0.5 mM ATP) for 1 hr at room temperature. After centrifugation at 100,000 × *g* at 25°C for 30 min in a Beckman TLA 100.3 rotor, pellets and supernatants were separated immediately. Each pellet was then washed gently with 200 μl of liposome binding buffer and resuspended in an equal volume of supernatant. All fractions were analyzed by SDS-PAGE followed by Coomassie staining.

In Vitro Reconstitution of Clathrin Buds

Aliquots of autolysosomes were added to binding reactions containing rat brain cytosol pre-treated with anti-GFP (400 μg/ml) and anti-clathrin heavy-chain (400 μg/ml) antibodies as indicated at 4°C for 1.5 hr, an ATP regeneration system, and 5 μg of KIF5B. The mixture was incubated at 37°C for 1 hr and the reactions were terminated by chilling on ice. After centrifugation, the reconstituted autolysosomes were collected by centrifugation.

In Vitro Reconstitution of Autolysosome Tubulation

The in vitro reconstitution of autolysosome tubulation was done as previously described (Su et al., 2016; Wang et al., 2015). The tubulation assay chambers were prepared as for the gliding assay. The channels were sequentially coated with 10 μg/ml anti-tubulin antibody and 3 mg/ml casein, allowing microtubules to be immobilized on the coverslips. For tubulation of PtdIns(4,5)P_2-containing liposomes, 80 nM full-length KIF5B was incubated with 28 μg/ml 5% PtdIns(4,5)P_2-containing liposomes. For autolysosome tubulation, 80 nM full-length KIF5B was incubated with ~0.3 mg/ml autolysosomes, which were treated by different methods including trypsin digestion and cytosol incubation. The motor-coated vesicles were introduced into the microtubule-coated flow chambers, then 60 μl of solution containing 20 μM ATP, 1 mg/ml casein, 10 mM DTT, 5% glucose, 600 μg/ml glucose oxidase, 60 μg/ml catalase, and an ATP regeneration system and an oxygen scavenger system were added to the chambers. The formation of tubules was visualized using a Nikon TIRF microscope. The fluorescent labeled protein is labeled according to the previous study by Bates et al. (2007).

Field Emission In-Lens Scanning Electron Microscopy

Autolysosomes were incubated on glass chips at 37°C for 1 hr, then fixed with 2% glutaraldehyde in PBS buffer at room temperature for 30 min. The samples were then rinsed and post-fixed with 1.0% OsO_4 in 0.1 M sodium cacodylate buffer at room temperature for 20 min. After dehydration in a graded ethanol series (30%, 50%, 70%, 90%, 100%, and 100%, 10 min each), the samples were transferred to Arklone for critical point drying using highest-purity CO_2 in a Hitachi HCP-2 Critical Point Dryer. The samples were then coated with 4 nm gold in a Hitachi E-1045 ion sputter coater and viewed with an S4800 Hitachi scanning electron microscope at 6 kV accelerating voltage.

Lipid Overlay Assay

Nonspecific binding sites on the lipid strips were first blocked with 10% (w/v) milk powder. The membranes were incubated for 1 hr at room temperature with purified KIF5B (2 μg/ml in PBS containing 10% milk and 0.1% Tween 20). The blots were washed in PBS containing 0.1% Tween 20 and incubated with a rabbit anti-KIF5B antibody (Abcam). After washing, the blots were incubated with anti-rabbit antibody conjugated to horseradish peroxidase, and visualization was carried out using enhanced chemiluminescence.

Liposome Flotation Assay

Protein (2 μM) and lipids (800 μM) were incubated at room temperature for 1 hr. A sucrose gradient (20 mM Tris-HCl [pH 8.0], 150 mM NaCl) containing 200 μl of the sample mixed with 200 μl of 60% sucrose, 400 μl of 25% sucrose, 400 μl of 20% sucrose, and 200 μl of buffer was constructed. Fractions of 100 μl were collected after ultracentrifugation in an MLS-50 rotor (Beckman) at 35,000 rpm for 2 hr. Fractions were run on SDS-PAGE gels followed by Coomassie staining.

Statistics

Experimental groups were compared using two-tailed t tests.

SUPPLEMENTAL INFORMATION

Supplemental Information includes Supplemental Experimental Procedures, six figures, and one movie and can be found with this article online at http://dx.doi.org/10.1016/j.devcel.2016.04.014.

AUTHOR CONTRIBUTIONS

L.Y. and Y.J.S. conceived the idea. L.Y. and Y.J.S. supervised the study with help from W.Q.D., Q.P.S., and Y.C. W.Q.D., Q.P.S., and Y.C. designed and conducted most of the experiments and analyzed the data. Y.Y.Z., D.J., Y.G.R., S.Y.Z., Y.X.Z., H.R., C.M.Z., X.Q.W., N.G., Y.F.W., and L.F.S. contributed to the ideas and experiments. L.Y. wrote the manuscript.

ACKNOWLEDGMENTS

We are grateful to Nikon Instruments (Shanghai) and the Tsinghua Cell Biology Core Facility for providing technical support. This research was supported by the National Natural Science Foundation of China 31430053 and 31321003, Natural Science Foundation of China international cooperation and exchange program 31561143002, Beijing Natural Science Foundation 5142011, International Cooperation Grant of Science and Technology 2014DFG32460, National Science Foundation of China 21573013, 21390412, 31271423, and 31327901, 863 Program SS2015AA020406, and CAS Interdisciplinary Innovation Team for Y.S.

Received: September 15, 2015
Revised: January 14, 2016
Accepted: April 20, 2016
Published: May 23, 2016

REFERENCES

Bates, M., Huang, B., Dempsey, G.T., and Zhuang, X. (2007). Multicolor super-resolution imaging with photo-switchable fluorescent probes. Science *317*, 1749–1753.

Campas, O., Leduc, C., Bassereau, P., Casademunt, J., Joanny, J.-F., and Prost, J. (2008). Coordination of kinesin motors pulling on fluid membranes. Biophys. J. *94*, 5009–5017.

Cardoso, C.M., Groth-Pedersen, L., Hoyer-Hansen, M., Kirkegaard, T., Corcelle, E., Andersen, J.S., Jaattela, M., and Nylandsted, J. (2009). Depletion of kinesin 5B affects lysosomal distribution and stability and induces peri-nuclear accumulation of autophagosomes in cancer cells. PLoS One *4*, e4424.

Collins, B.M., McCoy, A.J., Kent, H.M., Evans, P.R., and Owen, D.J. (2002). Molecular architecture and functional model of the endocytic AP2 complex. Cell *109*, 523–535.

Dabora, S.L., and Sheetz, M.P. (1988). The microtubule-dependent formation of a tubulovesicular network with characteristics of the ER from cultured cell extracts. Cell *54*, 27–35.

Friedman, D.S., and Vale, R.D. (1999). Single-molecule analysis of kinesin motility reveals regulation by the cargo-binding tail domain. Nat. Cell Biol. *1*, 293–297.

Hirokawa, N., and Noda, Y. (2008). Intracellular transport and kinesin superfamily proteins, KIFs: structure, function, and dynamics. Physiol. Rev. *88*, 1089–1118.

Honing, S., Ricotta, D., Krauss, M., Spate, K., Spolaore, B., Motley, A., Robinson, M., Robinson, C., Haucke, V., and Owen, D.J. (2005). Phosphatidylinositol-(4,5)-bisphosphate regulates sorting signal recognition by the clathrin-associated adaptor complex AP2. Mol. Cell *18*, 519–531.

Kano, F., Sako, Y., Tagaya, M., Yanagida, T., and Murata, M. (2000). Reconstitution of brefeldin A-induced Golgi tubulation and fusion with the endoplasmic reticulum in semi-intact Chinese hamster ovary cells. Mol. Biol. Cell *11*, 3073–3087.

Kaufmann, A., Beier, V., Franquelim, H.G., and Wollert, T. (2014). Molecular mechanism of autophagic membrane-scaffold assembly and disassembly. Cell *156*, 469–481.

Klopfenstein, D.R., Tomishige, M., Stuurman, N., and Vale, R.D. (2002). Role of phosphatidylinositol(4,5)bisphosphate organization in membrane transport by the Unc104 kinesin motor. Cell *109*, 347–358.

Koster, G., VanDuijn, M., Hofs, B., and Dogterom, M. (2003). Membrane tube formation from giant vesicles by dynamic association of motor proteins. Proc. Natl. Acad. Sci. USA *100*, 15583–15588.

Leduc, C., Campas, O., Zeldovich, K.B., Roux, A., Jolimaitre, P., Bourel-Bonnet, L., Goud, B., Joanny, J.-F.o., Bassereau, P., and Prost, J. (2004). Cooperative extraction of membrane nanotubes by molecular motors. Proc. Natl. Acad. Sci. USA *101*, 17096–17101.

Luzio, J.P., Pryor, P.R., and Bright, N.A. (2007). Lysosomes: fusion and function. Nat. Rev. Mol. Cell Biol. *8*, 622–632.

McMahon, H.T., and Boucrot, E. (2011). Molecular mechanism and physiological functions of clathrin-mediated endocytosis. Nat. Rev. Mol. Cell Biol. *12*, 517–533.

Miki, H., Okada, Y., and Hirokawa, N. (2005). Analysis of the kinesin superfamily: insights into structure and function. Trends Cell Biol. *15*, 467–476.

Mizushima, N. (2007). Autophagy: process and function. Genes Dev. *21*, 2861–2873.

Mousavi, S.A., Malerod, L., Berg, T., and Kjeken, R. (2004). Clathrin-dependent endocytosis. Biochem. J. *377*, 1–16.

Rong, Y., McPhee, C.K., Deng, S., Huang, L., Chen, L., Liu, M., Tracy, K., Baehrecke, E.H., Yu, L., and Lenardo, M.J. (2011). Spinster is required for autophagic lysosome reformation and mTOR reactivation following starvation. Proc. Natl. Acad. Sci. USA *108*, 7826–7831.

Rong, Y., Liu, M., Ma, L., Du, W., Zhang, H., Tian, Y., Cao, Z., Li, Y., Ren, H., Zhang, C., et al. (2012). Clathrin and phosphatidylinositol-4,5-bisphosphate regulate autophagic lysosome reformation. Nat. Cell Biol. *14*, 924–934.

Roux, A., Cappello, G., Cartaud, J., Prost, J., Goud, B., and Bassereau, P. (2002). A minimal system allowing tubulation with molecular motors pulling on giant liposomes. Proc. Natl. Acad. Sci. USA *99*, 5394–5399.

Royle, S.J., Bright, N.A., and Lagnado, L. (2005). Clathrin is required for the function of the mitotic spindle. Nature *434*, 1152–1157.

Su, Q.P., Du, W., Ji, Q., Xue, B., Jiang, D., Zhu, Y., Lou, J., Yu, L., and Sun, Y. (2016). Vesicle size regulates nanotube formation in the cell. Sci. Rep. *6*, 24002.

Tanaka, Y., Kanai, Y., Okada, Y., Nonaka, S., Takeda, S., Harada, A., and Hirokawa, N. (1998). Targeted disruption of mouse conventional kinesin heavy chain, kif5B, results in abnormal perinuclear clustering of mitochondria. Cell *93*, 1147–1158.

Vale, R.D., and Hotani, H. (1988). Formation of membrane networks in vitro by kinesin-driven microtubule movement. J. Cell Biol. *107*, 2233–2241.

Vale, R.D., Reese, T.S., and Sheetz, M.P. (1985). Identification of a novel force-generating protein, kinesin, involved in microtubule-based motility. Cell *42*, 39–50.

Venkateswarlu, K., Hanada, T., and Chishti, A.H. (2005). Centaurin-alpha1 interacts directly with kinesin motor protein KIF13B. J. Cell Sci. *118*, 2471–2484.

Wang, C., Du, W., Su, Q.P., Zhu, M., Feng, P., Li, Y., Zhou, Y., Mi, N., Zhu, Y., Jiang, D., et al. (2015). Dynamic tubulation of mitochondria drives mitochondrial network formation. Cell Res. *25*, 1108–1120.

Yu, L., McPhee, C.K., Zheng, L., Mardones, G.A., Rong, Y., Peng, J., Mi, N., Zhao, Y., Liu, Z., Wan, F., et al. (2010). Termination of autophagy and reformation of lysosomes regulated by mTOR. Nature *465*, 942–946.

Zhou, Y., Zhu, S., Cai, C., Yuan, P., Li, C., Huang, Y., and Wei, W. (2014). High-throughput screening of a CRISPR/Cas9 library for functional genomics in human cells. Nature *509*, 487–491.